Effect of dynamic loading on ductile crack initiation behaviour of notched specimen with strength mismatch

G.-B. An*[1], M. Ohata[2], J.-U. Park[3] and M. Toyoda[2]

The present study focuses on the effects of a geometrical discontinuity, strength mismatching, which can increase plastic constraint due to heterogeneous plastic straining, and the loading rate on the critical condition for ductile fracture initiation using a two-parameter criterion based on equivalent plastic strain and stress triaxiality. Fracture initiation testing was conducted under dynamic loading using circumferentially notched bend specimens. In order to evaluate the condition for the ductile crack initiation state in the specimens, a thermal elastic/plastic dynamic finite element analysis considering the temperature increase due to plastic deformation was performed. The two-parameter criterion was shown to be applicable to ductile cracking from the surface of the prenotched root in the strength mismatched specimen under dynamic bend loading.

Keywords: Ductile crack initiation, Dynamic loading, Plastic constraint, Strength mismatch, Stress triaxiality

Introduction

Brittle failure of high toughness steel structures tends to occur after ductile crack initiation/propagation. An example is the damage to steel structures in the Hanshin Great Earthquake in Japan.[1–3] Several brittle failures were observed in the beam-to-column connection zones, which have geometrical discontinuity. In some of these zones, brittle fractures occurred after large scale plastic deformation associated with ductile crack initiation and extension from stress–strain concentrators. This earthquake, in particular, led to brittle failures of steel structures under high speed ground motion (104 cm s^{-1}) and significantly large ground displacement (27 cm).

The integrity of steel framed structures under earthquake induced large scale deformation and a high speed loading rate can be evaluated by estimating ductile crack initiation and propagation, followed by brittle fracture. Based on ductile crack initiation behaviour, the ductile cracking controlling mechanical parameters can be expressed in terms of two parameters, i.e. equivalent plastic strain $\bar{\varepsilon}p$ and stress triaxiality $\sigma m/\bar{\sigma}$ (σ_m=mean stress, $\bar{\sigma}$ =Von Mises equivalent stress).[4] Ductile crack initiation has been shown in experiments using circumferentially notched bend specimens. A welded joint in a steel structure exhibits not only geometrical heterogeneity, but also strength mismatching. As the existence of strength mismatch leads to more plastic constraints in the lower strength regions,[5–7] it can be assumed that the ductile fracture initiation behaviour is also influenced by strength mismatch. In addition, it has been reported that the mechanical properties of steels change under dynamic loading,[8] and the strain rate effect on mechanical properties also depends on the strength level of steel.[9]

The present study focuses on fundamentally clarifying the effect of the loading rate on the critical conditions for initiating ductile fracture from the notch root with strength mismatch. The behaviour of ductile crack initiation from the prenotched root of Charpy type specimens with the strength mismatch effect of dynamic loading was investigated by bending tests. Moreover, in order to evaluate the ductile crack initiation behaviour in the specimens under dynamic loading, thermal elastic/plastic dynamic finite element (FE) analyses, considering the temperature rise due to adiabatic plastic deformation, were carried out. Finally, it is shown that the condition for ductile crack initiation using the two parameters of equivalent plastic strain and stress triaxiality can be a transferable criterion for the evaluation of ductile crack initiation from the surface of a prenotched root.

Criterion for ductile crack initiation from prenotched root surfaces and the effect of strength mismatching and dynamic loading

The critical condition for the formation of ductile cracks from the surface of a prenotched root was estimated by using Charpy type bend specimens with a sharp V-type notch under dynamic loading. Also, the effect of

[1]Institute of Industrial Technology, Welding Research Part, Geoje Shipyard, Samsung Heavy Industries Co., Ltd., 530, Jangpyung-Ri, Sinhyun-Up, Geoje, Gyeongsangnam-Do 656-710, Korea
[2]Department of Manufacturing Science, Graduate School of Engineering, Osaka University, 2-1, Yamada-oka, Suita, Osaka 565-0871, Japan
[3]Department of Civil Engineering, Chosun University, 375, Seosek-dong, Dong-Gu, Gwangju, 501-759, Korea

*Corresponding author, email gyubaek.an@samsung.com

Published by Maney on behalf of the Institute
Received 25 February 2005; accepted 15 September 2005
DOI 10.1179/174329306X77894

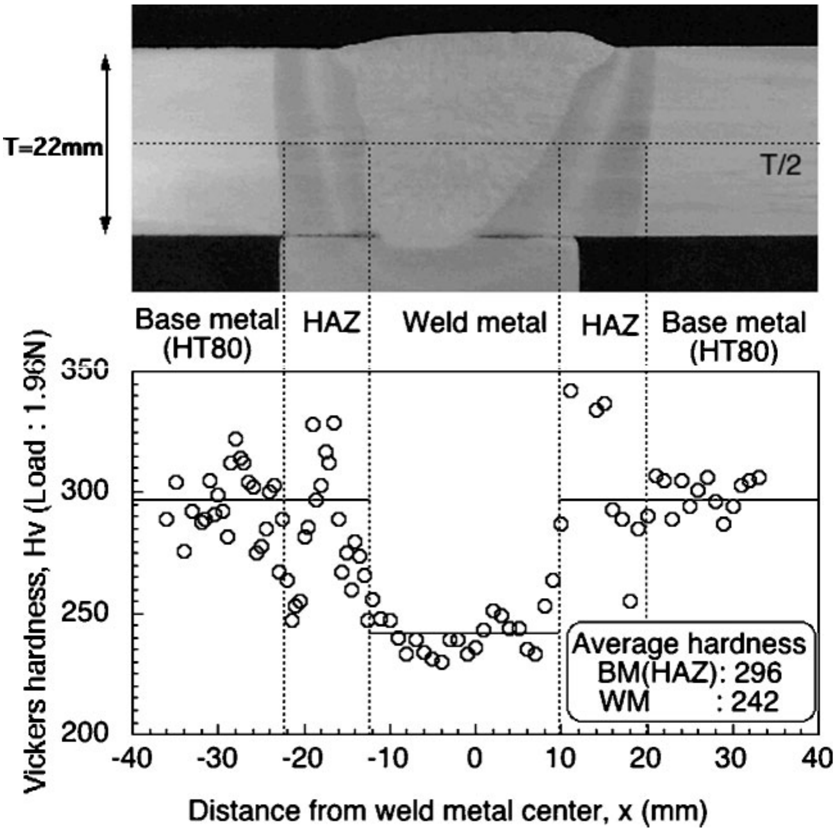

1 Vickers hardness distribution of welded joint

strength mismatching near the prenotched root on ductile crack initiation was investigated.

Three-point bending test

The strength mismatch welded joint was made by electrogas welding using a welding wire for 500 MPa class steel and a 22 mm thick HT80 steel plate as the base metal. The chemical compositions of the base metal and mechanical properties of the weld metal and base metal are shown in Tables 1 and 2, respectively. This welded joint is a strength mismatch joint with strength ratio of yield stress (S_r(Y)) and tensile strength (S_r(T)) of approximately 1·7 and 1·3, respectively. A micrograph of the joint and the Vickers hardness distribution near the welded joint in the thick central part of the plate are shown in Fig. 1.

The characteristics of ductile crack initiation from the surface of a prenotched root and the effects of strength mismatch were investigated using a Charpy type bend specimen. Figure 2 presents the configurations of two types of three-point bend test specimens used. One is a strength mismatched specimen in which a notch tip is located at the fusion line of a welded joint, while the other is a homogeneous specimen with a notch in the centre of the weld metal.

The three-point bending test was carried out by using the servohydraulic high loading rate bending test machine on the homogeneous and mismatched Charpy type specimens with a sharp V-type notch (R=0·25 mm). The bending tests were carried out at a crosshead displacement speed of 10 mm s^{-1}. To clarify the load levels of ductile crack initiation from the surface of the prenotched root, unloading tests were carried out at various loading levels before failure. After loading, each specimen was cut longitudinally through its centre. One side of the specimen was used for observing crack

Table 1 Chemical composition of base metal (HT80 steel) used

Steel	C	Si	Mn	P	S	Cu	Cr	Mo	V	Ti	Nb	Al	Ni	B	C_{eq}	P_{cm}
HT80	0·10	0·26	0·85	0·004	0·002	0·23	0·49	0·47	0·037	0·016	0·011	0·046	1·16	0·0012	0·50	0·25

C_{eq}=C+Mn/6+(Cr+Mo+V)/5+(Cu+N)/15
P_{cm}=C+Si/30+Mn/20+Cu/20+Ni/60+Cr/20+Mo/15+V/10+5B

Table 2 Mechanical properties of weld metal and base metal used

Material	σ_Y, MPa	σ_T, MPa	YR	S_r (Y)	S_r (T)	ε_T, %	EL, %
Base metal (BM)	846	887	96	1·67	1·31	6·0	30·8
Weld metal (WM)	509	672	76	1·67	1·31	11·4	32·0

σ_Y=lower yield stress, σ_T=tensile strength, YR=yield-to-tensile ratio (σ_Y/σ_T), ε_T=uniform elongation, EL=elongation (gage length=12 mm, diameter=6 mm), $S_r(Y)=\sigma_Y^{BM}/\sigma_Y^{WM}$, $S_r(T)=\sigma_T^{BM}/\sigma_T^{WM}$

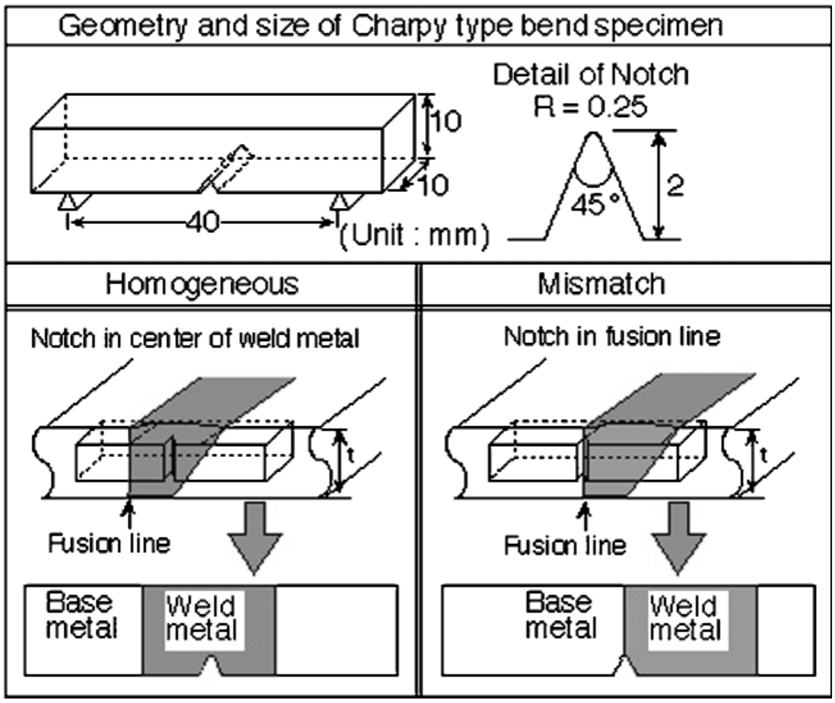

2 Geometry and size of a three-point bend specimen

initiation behaviour, while the other side was subjected to brittle fracture using liquid nitrogen, to compare the ductile fracture surface characteristics according to ductile crack initiation.

Influence of the strength mismatching on ductile crack initiation behaviour under dynamic loading

Figures 3 and 4 show the relationship between load P and displacement of crosshead D_y, and the SEM observation results near the prenotched root tip at the middle section of homogeneous and mismatched specimens under dynamic loading. Ductile crack initiation behaviour, i.e. initiation from the prenotched root surface along the shear band in the weld metal, was the same as that for the static load.[10] In addition, Fig. 5 shows the comparison of the ductile crack initiation at level 1 in Fig. 3 with the fracture surface, which showed brittle fracture resulting from the use of liquid nitrogen after unloading level 1. The dimple was observed near the prenotched root in the fracture surface. Also, these results are very similar to those of homogeneous specimens under dynamic loading. No significant difference is observed in the ductile crack initiation behaviour between homogeneous and mismatched specimens under dynamic loading.

Applicability of two-parameter criterion effect of dynamic loading with strength mismatched specimens

The dependence of triaxial stress state on ductile crack initiation in materials has been widely expressed by using two parameters, equivalent plastic strain and stress triaxiality.[4]

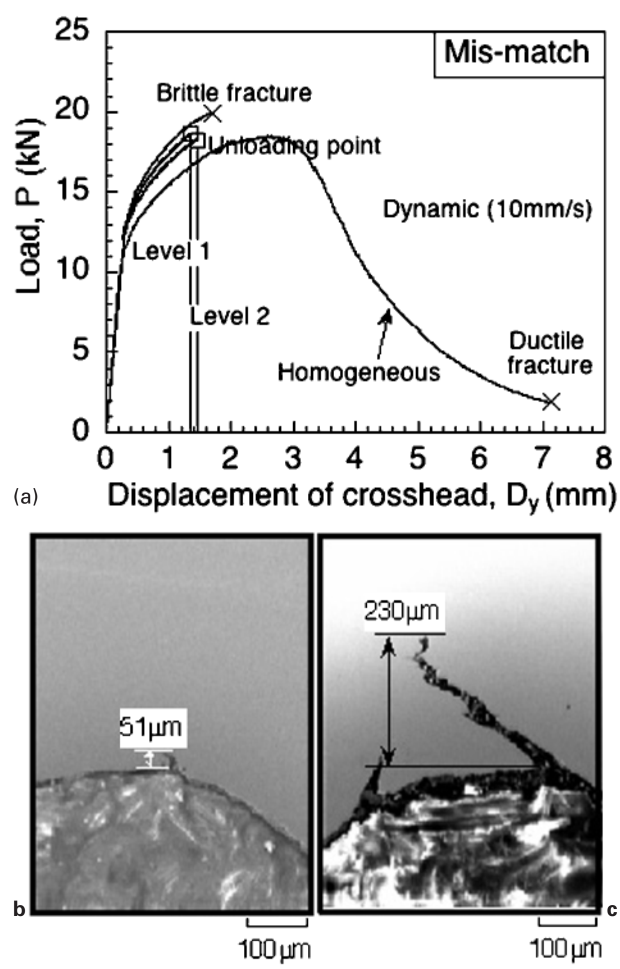

a P–D curves; *b* at level 1; *c* at level 2

3 Ductile crack initiation behaviour of mismatched specimens under dynamic loading

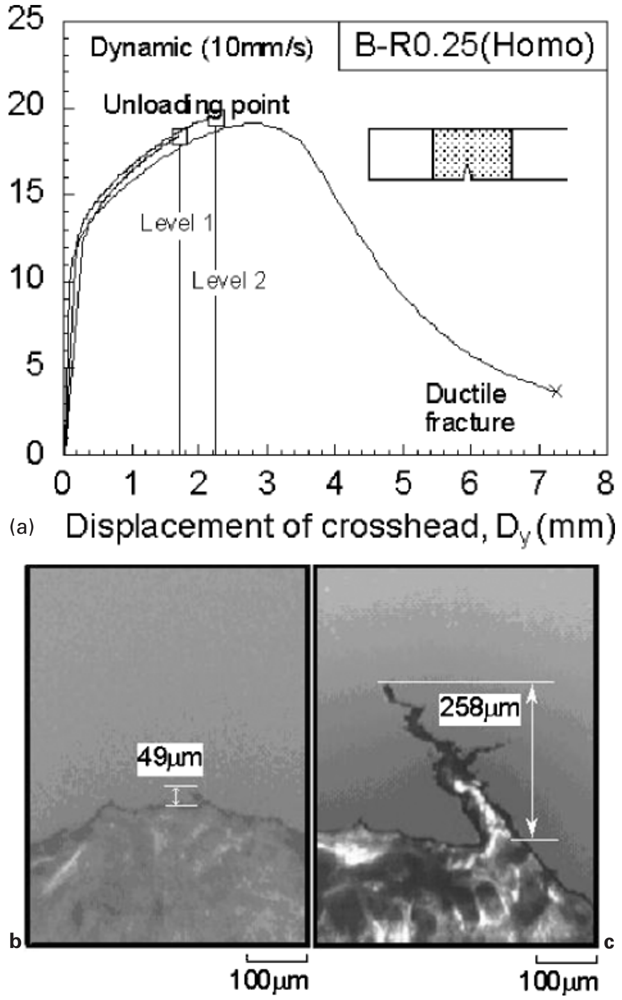

a P–D curves; *b* at level 1; *c* at level 2

4 Ductile crack initiation behaviour of homogeneous specimens under dynamic loading

Numerical analysis

The coupled heat conduction and elastic/plastic dynamic FE analyses were used for analysing the stress–strain behaviours of homogeneous and mismatched specimens. Figure 6 shows the mesh division used in these analyses. The geometry and dimensions of the bend models are the same as those used in the bend test.

The most important aspect in analysis is employing the proper material constitutive equation, especially for a dynamic loaded specimen which produces a temperature rise during the loading. The authors have suggested a simple and correct method for analysing the stress–strain state at a local area in the specimen at current temperature and strain rate during dynamic loading.[11] This method is based on using the so-called strain rate–temperature parameter R,[12,13] which was originally proposed for the characterisation of the effect of strain rate and test temperature on yield stress σ_Y.[14] The tensile strength σ_T is also characterised by using the modified R parameter, taking into account the temperature rise ΔT, which is generated by adiabatic plastic strain up to the applied stress σ_T, since the stress σ_T obtained with tensile testing under dynamic loading cannot be the stress at the initial specimen temperature.[15] The modified R parameter used is defined as follows

$$R=(T+\Delta T)\ln(A/\varepsilon) \quad (1)$$

where ε is strain rate, T is test temperature (initial specimen temperature), ΔT is temperature rise, and A is material constant. The FE analysis taking into account heat generation and conduction was carried out using the finite element code ABAQUS version 5.8.[16] In this coupled thermal elastic/plastic FE analysis, 90% of the plastic work generated was assumed to be converted into heat, causing a temperature rise.[17–19] The physical properties shown in Table 3 were used for heat conduction and thermal stress analysis.

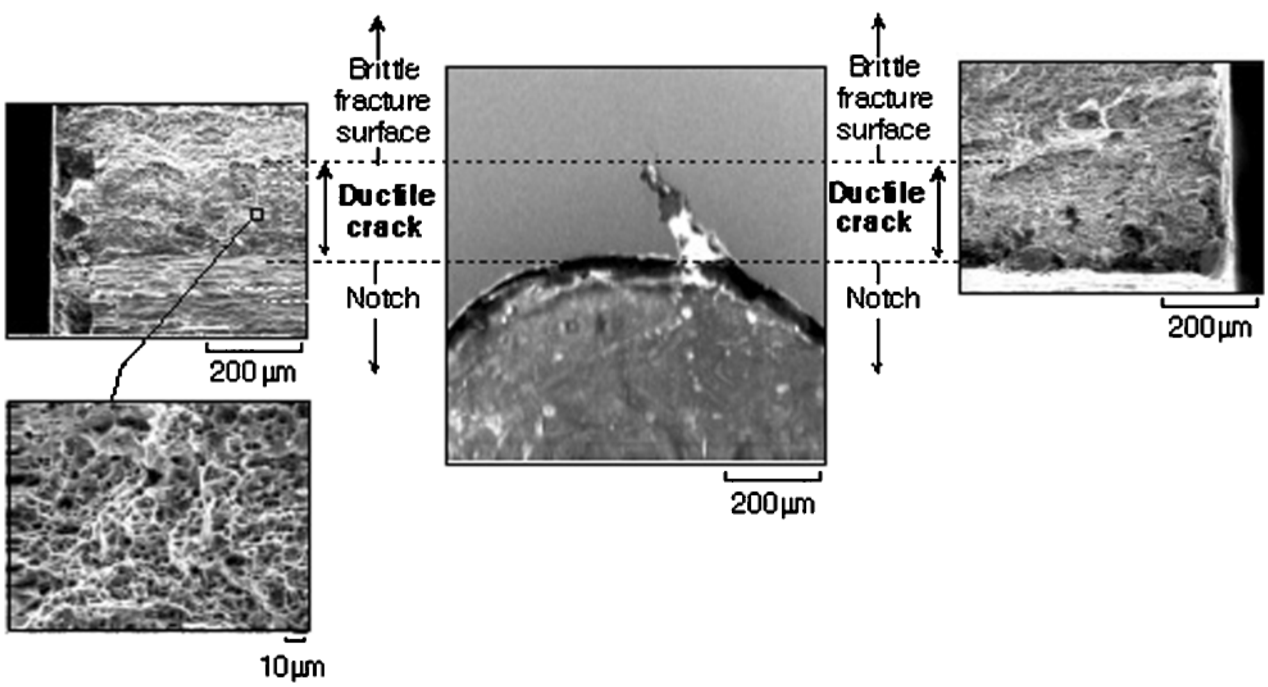

5 Fractography near the ductile crack initiation region and brittle fracture region in mismatch specimen under dynamic loading

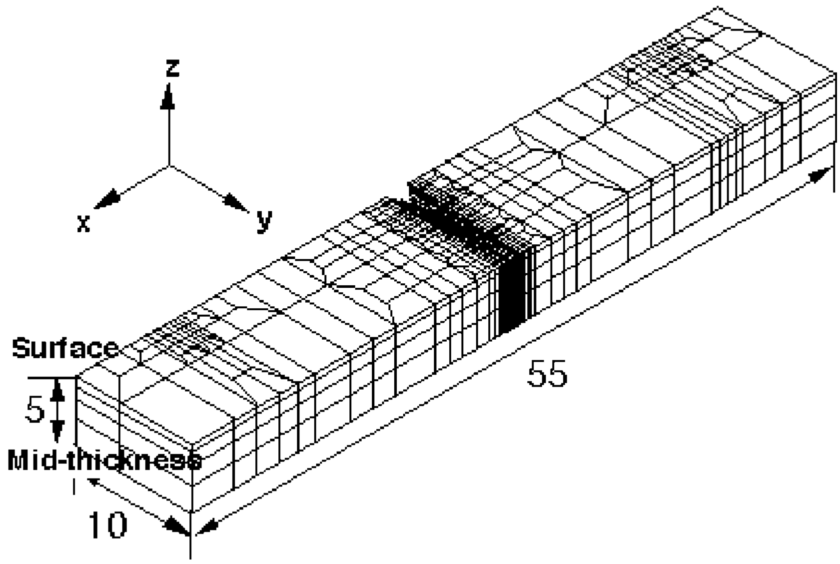

6 Mesh division of a three-point bend specimen used for FE analysis

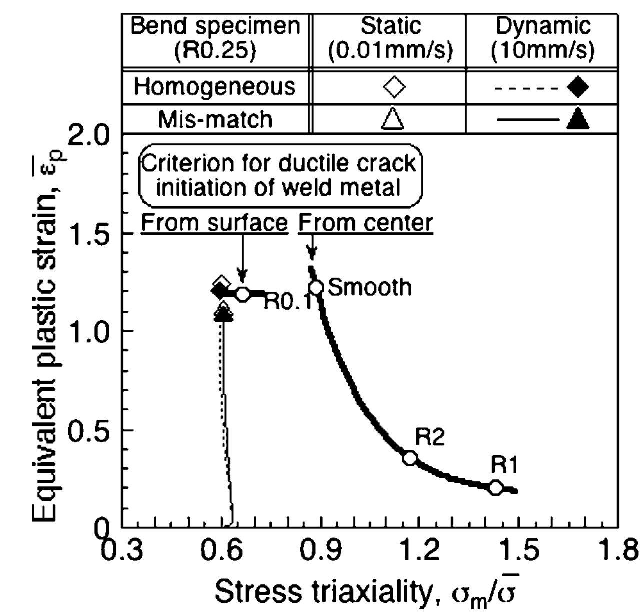

7 Condition for ductile crack initiation using the two parameters equivalent plastic strain $\bar{\varepsilon}_p$ and stress triaxiality $\sigma_m/\bar{\sigma}$, for homogeneous and mismatched specimens under dynamic loading

Effect of dynamic loading on the critical conditions for ductile crack initiation of specimen with strength mismatch

The effect of dynamic loading on the critical condition for ductile crack initiation of mismatch specimens was investigated by carrying out FE analyses.

Figure 7 shows the history of the equivalent plastic strain and stress triaxiality relationship at ductile crack initiation for the surface of the prenotched root as the maximum strain element for homogeneous and strength mismatched specimens under dynamic bend loading. Strength mismatching did not affect the history of the $\bar{\varepsilon}p-\sigma m/\bar{\sigma}$ relation. In addition, the critical value of the strength mismatched specimen was also slightly lower than that of the homogeneous specimen. However, the criterion was expressed as the critical value of a homogeneous round bar tensile specimen. Consequently, by conducting the coupled heat conduction and elastic/plastic FE analyses, the two-parameter criterion can be shown to be applicable to the ductile cracking initiation from the surface of a prenotched root in the strength mismatched specimen under dynamic loading. The results would be in accordance with the constant plastic strain condition of a surface cracking type of specimen.

Discussion

The strength mismatch cannot affect the change of failure mode but only the change of plastic constraint, which leads to different stress triaxiality when the loading mode is single bend. This result enables us to estimate the ductile crack initiation for strength mismatch specimens by using the two parameter criterion. It was found that the dynamic loading in single bend which produces the change of local strain rate also gave the same ductile crack criterion.

Conclusions

The transferability of local mechanical conditions for ductile cracking was examined in this study by investigating two parameters, i.e. equivalent plastic strain and

Table 3 Material constants used for coupled thermal elastic/plastic FE analysis

Material	E, MPa	ν	c, J kg^{-1} K^{-1}	ρ, kg mm^{-3}	κ, m^2 s^{-1}	β, K^{-1}
Base metal (BM) Weld metal (WM)	206	0·3	$4{\cdot}8\times10^{2}$	$8{\cdot}0\times10^{-6}$	$2{\cdot}17\times10^{-5}$	$1{\cdot}2\times10^{-5}$

E=Young's modulus, ν=Poisson's ratio, c=specific heat, ρ=density, κ=heat conductivity, β=coefficient of heat.

stress triaxiality, obtained from mismatched specimens with a prenotched root and under dynamic loading. The two parameter criterion was shown to be applicable to ductile cracking from the surface of the prenotched root in the strength mismatched specimen under dynamic bend loading based on the results obtained from conducting coupled heat conduction and elastic/plastic FE analyses considering the temperature rise. The results were in accordance with the constant plastic strain condition of surface cracking type specimens.

References

1. Reconnaissance Report of Hyogo-Nanbu (Hanshin/Awaji) Earthquake at 1995 in Japan, AIJ, Steel Committee of Kinki Branch, 1995 (in Japanese).
2. M. Toyoda: *Weld. J.*, 1995, **74**, 132–136.
3. K. Okashita, R. Ohminami, K. Michiba, A. Yamamoto, M. Tomimatsu, Y. Tanji and C. Miki: *J. Japan Soc. Civil Eng.*, 1998, **591**, **(I–43)**, 243–261 (in Japanese).
4. F. A. Mcclintock: *J. Appl. Mechanics Trans ASME*, 1968, **35**, 363–371.
5. K. Satoh and M. Toyoda: *J. Soc. Naval Architects Japan*, 1972, **132**, 381–393 (in Japanese).
6. M. Toyoda: Doctoral thesis, Osaka University, 1973, 10–15 (in Japanese).
7. M. Kocak, M. Pakdil and G. Cam: *Sci. Technol. Weld. Joining*, 2002, **7**, (4), 187–196.
8. A. R. Rosenfield and D. T. Hahn: *Trans. ASM*, 1966, **59**, 962–980.
9. N. Ishikawa, Y. Kobayashi and M. Toyoda: *Tetsu-To-Hagane*, 1998, **84**, 37–42 (in Japanese).
10. G.-B. An, M. Ohata and M. Toyoda: *Eng. Fracture Mechanics*, 2003, **70**, 1359–1377.
11. M. Toyoda, M. Mochizuki, T. Ohmura and G. B. An: Proc. Int. Seminar on 'Numerical analysis in solid and fluid dynamics', 217; 1999.
12. P. E. Bennet and G. M. Sinclair: *J. Basic Eng.*, 1961, **83**, 557–564.
13. P. E. Bennet and G. M. Sinclair: ASME Publication 65-MET11, 1965.
14. E. Fujii, I. Ohkuma, Y. Kawaguchi and M. Tsukamoto: *Soc. Naval Architects Japan*, 1985, **158**, 619–629 (in Japanese).
15. F. Minami, T. Ochiai, T. Hashida, K. Arimochi and N. Konda: *Fatigue Fracture Mechanics ASTM STP*, 2000, **31**, (1389), 271–304.
16. K. Hibbit: 'ABAQUS/Standard user's manuals', Ver. 5.8, Vol. 1–3; 1998, USA, Sorensen Inc.
17. U. S. Lindholm, A. Nagy, G. R. Johnson and J. M. Hoegfeldt: *J. Eng. Mater. Technol. ASME*, 1983, **102**, (4), 376–381.
18. M. R. Staker: *Acta Metall.*, 1981, **29**, (4), 683–689.
19. S. L. Semiatin, M. R. Staker and J. J. Jonas: *Acta Metall.*, 1984, **32**, (9), 1347–1354.